Rezvanifar and Vosoughifar
Journal of Engineering and Applied Science (2023) 70:31
https://doi.org/10.1186/s44147-023-00203-x

Journal of Engineering and Applied Science

RESEARCH Open Access

A modified NARX approach for evaluating the time history effect of climate change on load combination in designing façade structures

Mostafa Rezvanifar[1*] and Hamidreza Vosoughifar[2]

*Correspondence:
Mostafa.rezvanifar@gmail.com

[1] The University of South-Tehran Branch, ZIP Area 11, North Iranshahr Street, Tehran, Iran
[2] The University of Hawaii at Manoa, 2500 Campus Rd, Honolulu, HI 96822, USA

Abstract

In recent years, researchers, designers, and project owners have deemed the dry facade system to be a suitable option. Consequently, much research has been conducted on the structural behavior of the dry facade system when subjected to seismic loads, climate change, thermal loads, etc. Of particular concern is the destructive phenomenon of corrosion due to climate change in coastal areas which can damage the infrastructure of the dry façade. To address this issue, a modified NARX method was employed in this study to predict climate change variables for use in dry facade analysis. The author of this paper developed a flowchart and subroutines in MATLAB as a new toolbox for this purpose. Temperature was identified as the most influential parameter in consequent configurations and was thus considered in load combination for the design of a dry facade structure. The statistical results obtained from NARX showed good agreement with measured data; specifically, there was a low mean absolute error (MAE) of 0.345 °C, a low root-mean-square error (RMSE) of 0.442 °C, and a high coefficient of determination (R^2) of 0.998 (P-value = 0.918 > 0.05). Finally, this study proposed a modified formula for load combination to ensure durability and constructability of dry facades in coastal cities.

Keywords: Climate change, Artificial neural network, Building façades, Structure design, Load combination

Introduction

The global success of dry facade systems in the last decade has been attributed to several advantages, such as their lightweight, durability, and fast construction [1]. This system consists of a cold-formed structure (CFS) that is covered with suitable elements as a building façade [2]. However, climate change poses a significant risk to the safety and performance of dry facade systems. Recent assessments have reported that climate change is having a major impact on light and dry facade systems [3-5]. Unfortunately, there is limited information and fundamental research on adapting to climate change in the construction industry [6]. In buildings designed to meet current standards, future

maintenance costs will likely increase significantly due to the effects of climate change. To ensure current and future structures are able to withstand changes in wind speed, severe weather events, temperature fluctuations, rainfall patterns, and relative humidity levels, it is necessary to amend building codes accordingly. The building sector appears to be particularly vulnerable to the challenges posed by climate change, particularly global warming [7]. At the international level, however, due to a lack of effective work codes, limited progress has been made in assessing the preparedness of construction companies for this issue [6]. Moreover, in the dry façade design process, proper attention must be paid to corrosion as an important parameter in climate change [8]. Corrosion of offshore structures is inevitable due to the corrosiveness of seawater which has a significant impact on their strength and reliability [9]. Environmental effects can reduce material properties due to wave climate change and marine corrosion, pitting corrosion is particularly dangerous as it is a time-dependent mechanism [10]. The dry façade as a structural system is prone to corrosion and temperature changes, thus, changes in humidity can lead to its deterioration, especially in dry climates in tropical and coastal areas [11]. Design codes that take into account both local weather conditions and future change scenarios should be considered. These guidelines can be an important step towards a more proactive and dynamic approach towards ensuring high-quality production processes and creating a sustainable environment [12]. The consideration of a local climate that makes the dry facade resistant to future climate change is an important factor in building code [13]. In this regard, the load combination for the allowable stress design and strength design method [14] for the dry façade system was modified in this study to account for the impact of climate change. Specifically, the NARX method was employed to predict temperature using Ws, Td, RH, Tmin, and Tmax. Temperature, relative humidity, and dew point were identified as primary causes of barley corrosion [11]. Thus, in order to prevent future construction failure due to tangible climate change, it is suggested that activists and researchers in the construction industry consider this method when designing all aspects of construction in coastal areas. Consequently, a modified load combination with respect to the dry facade was proposed taking into account climate change variables.

Methods

Applying NARX results to the design process

Recently, artificial neural network (ANN)-based models have attracted researchers in various fields of construction due to their ability to obtain nonlinear relationships between inputs and outputs. Different ANN-based methods have been successfully applied to a variety of problems, such as flood [15], rainfall [16], water quality [17], and air temperature [18]. To address some of the issues associated with common ANN approaches, nonlinear autoregressive neural network with exogenous input (NARX was evaluated. NARX with recurrent dynamic networks has feedback connections with multiple different layers. The NARX model is a modification of the ARX model commonly used in time-series modeling [19]. The forward and backward processes between layers were designed for the NARX approach to make a multifaceted effort in simulating data [20]. The general structure of the NARX network is given by Eq. (1) [21]:

Table 1 NARX model specifications

Particulars	Configuration 1 to 9 specifications
Type of network	NARX neural network
Data division	Training 70%, 15% validation, and 15% testing
Training algorithm	Levenberg–Marquardt
Performance function	Mean squared error (*MSE*)
Optimized number of hidden neurons	3
Optimized number of delays	2

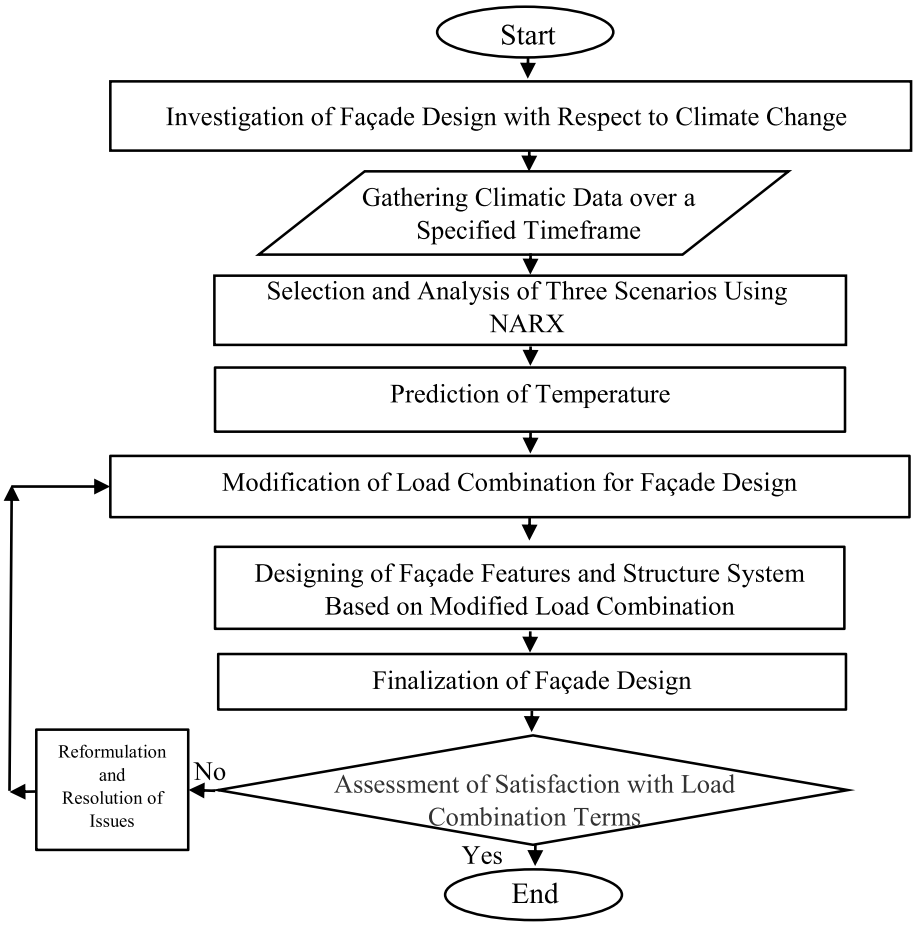

Fig. 1 Main flowchart of this study

$$y(t) = f(y(t-1), y(t-2), \ldots, y(t-ny), u(t-1), u(t-2), \ldots, u(t-nu)) \quad (1)$$

where y(t) is the predicted output trained based on the existing target value as the final network result [19, 22]. The specifications of the NARX model used in this study are summarized in Table 1. Figure 1 illustrates the flowchart steps of the study.

First, in order to assess the impact of climate change, it is necessary to determine the project plan according to climate change policies. Subsequently, data on climate change variables must be collected from reliable sources for 365 days for the considered cities. The input and

output data were then categorized into three scenarios and analyzed using the NARX method to predict the ideal temperature based on the history of temperature. To account for temperature in load combination evaluation, the predicted temperature was replaced with a "T" term in the equation. This resulted in an improved load combination equation. Finally, after producing materials based on this equation, it must be determined whether they meet the criteria of climate change, and if not, reforms and problem-solving measures must be taken.

Common load combinations for the design process are outlined in Table 2.

By substituting the temperature predicted from this step into the load combination equation, an improvement in the load combination equation can be achieved. Finally, after producing materials based on this step, it is necessary to ascertain whether they meet the criteria of climate change. When interpreting future weather forecasts, numerous uncertainties must be taken into account.

Climate change scenarios

Climate change scenarios are utilized to explore how the future will develop under a variety of alternative conditions or how to attain optimal results and avert unfavorable outcomes [23, 24]. Narrative descriptions of future events or weather patterns can be incorporated into the scenarios to enhance the consideration of extreme events [25]. Numerous uncertainties must be taken into account when interpreting future weather forecasts. On the other hand, to mitigate the effects of climate change on buildings, regional climate change must be taken into consideration [7]. Therefore, in this study, three scenarios were proposed with nine configurations. Scenario 1 included Ws, RH, Td, Tmin, and Tmax as input data and T as output data. Relative humidity was chosen as the target, and Ws, T, Td, Tmin, and Tmax were selected as inputs in scenario 2. In scenario 3, Ws, T, RH, Tmin, Tmax, and Td were chosen as inputs and output data, respectively.

Four statistical metrics were utilized in this study to evaluate the performance of the NARX model in predicting targets. These metrics include the mean absolute error (MAE), root-mean-square error (RMSE), correlation coefficient (R^2), and P-value. These criteria are commonly used statistical measurements to assess the accuracy of predictive models, as noted by Bateni, Vosoughifar, and Ek et al. [26].

$$MAE = \frac{1}{N}\sum_{i=1}^{N}|O_i - P_i| \tag{2}$$

$$RMSE = \sqrt{\frac{\sum_{i=1}^{N}(O_i - P_i)^2}{N}} \tag{3}$$

$$R^2 = \frac{\sum_{i=1}^{N}(O_i - \overline{O})(P_i - \overline{P})}{\sqrt{\sum_{i=1}^{N}(O_i - \overline{O})^2 \sum_{i=1}^{N}(P_i - \overline{P})^2}} \tag{4}$$

Table 2 Load combination formula based on *ASCE*

Term	Design method	Chapter of *ASCE*
$1.2D + 1.2T_1 + 0.5L$	LRFD	C2.3.4 P:419
$1.2D + 1.6L + 1.0T_1$	LRFD	C2.3.4 P:419
$1D + 1.0T_1$	ASD	C2.4.4 P:421
$1.0D + 0.75(L + T_1)$	ASD	C2.4.4 P:421

The *P*-value is a probability measure that ranges from 0 to 1. When this value falls below 0.05, it indicates a significant difference between two data sets [27, 28].

Case study

This study focuses on several case studies in coastal cities to evaluate the impact of climate change on dry facades. Figure 2 a, b, and c depicts the selected coastal cities for analysis purposes. The number of meteorological stations in Western Australia, California, and Iran is two, eighteen, and nine, respectively. Daily weather data from these stations were obtained from sources such as evapotranspiration for Western Australia [29], CIMIS for California [30], and I.R. of Iran Meteorological Organization (IRIMO) | E-Library [31] for Iran to obtain the best climate change scenarios.

Table 3 summarizes the mean value and standard deviation of each selected station's climatic data for analysis purposes.

Table 4 summarizes the geographical locations of the selected weather stations [32].

a. Australia **b.** California **c.** Iran

Fig. 2 The location of case studies. **a** Australia. **b** California. **c** Iran

Table 3 The mean (μ) and standard deviation (σ) values were calculated for each selected coastal station

No	City name	T (C^o)		T_{min}(C^o)		T_{max}(C^o)		W (m/s)		RH (%)		T_d(C^o)	
		μ	σ	μ	σ	μ	σ	μ	σ	μ	σ	μ	σ
1	Abadan	26.3	9.6	18.9	8.2	33.6	11.4	3.2	1.9	64.7	9.1	19.2	8.6
2	Ahvaz	26.6	9.6	19.4	8.3	33.7	11.1	2.4	1.5	65.6	7.8	19.6	8.9
3	Bandar Abas	27.5	5.8	23.4	6.8	31.6	5.9	3.7	1.2	78.6	7.9	22	6.9
4	Bandar Lengeh	27.2	5.8	21.9	6.2	32.5	5.6	3.7	1.8	73.2	5.4	23.3	6.3
5	Bushehr	25.3	7.2	20.6	7.1	29.9	7.6	3.5	1.9	75.8	6.9	20.1	7.1
6	Gorgan	18.2	8.2	12.9	8.1	23.4	8.9	2.6	1.4	63.6	14.3	11	7.1
7	Rasht	16.6	7.5	12.3	7.3	20.9	8.3	1.6	1.4	76.5	10.6	11.1	7.4
8	Sari	18.0	7.5	13.5	7.6	22.5	8.1	2.2	1.1	75.6	10.1	13.7	7.7
9	Kish Island	27.7	5.4	24.3	5.2	31.4	5.8	3.9	1.5	65.3	10.9	20.1	6.2
10	Atascadero	14.1	5.6	5.8	5.2	24.2	6.9	1.2	0.3	64.2	14.4	3.4	4.3
11	King City-Oasis	14.4	4.8	6.7	4.0	25.3	5.9	2.3	0.8	63.7	12.1	3.3	4.2
12	Lompoc	13.3	3.4	6.9	4.6	20.2	3.9	2.3	0.8	76.9	9.2	2.4	3.1
13	Long Beach	17.3	4.8	11.6	5.7	24.3	5.3	1.2	0.3	70.6	13.2	4.9	5.8
14	Santa Barbara	17.0	3.8	11.7	3.9	23.3	6.7	1.3	0.3	66.6	16.0	4.2	5
15	Sanel Valley	15.6	5.6	6.1	4.8	24.8	7.3	1.6	0.5	56.3	24.6	5.8	7.5
16	Santa Maria II	15.0	3.4	9.5	4.2	22.1	4.3	1.6	0.4	73.0	11.3	3.4	4.2
17	Santa Monica	18.1	3.8	13.9	4.0	23.3	4.4	1.7	0.3	68.1	17.7	4.2	5.1
18	Torry Pines	15.7	2.9	12.4	3.3	19.3	3.2	1.8	0.6	82.0	18.6	3.5	4.4
19	Watsonville West II	18.1	3.8	9.7	3.8	19.0	4.0	2.2	0.5	77.2	10.8	3	3.8
20	Diamond Springs	16.1	6.9	10.5	6	22.4	7.8	1.7	0.4	49.9	18.4	6.1	4.8
21	Woodland	17.1	6.2	9.8	5	25.3	8	2.2	0.9	54.8	16.3	8	4.6
22	Bishop	13.5	8	2.6	7.2	23.5	8.1	1.6	0.5	33.8	11.8	0.2	7.4
23	Gilroy	14.8	4.8	7.5	5.1	23.8	6.2	2.2	0.7	66.9	12.1	8.2	4.3
24	Delano	17.6	8.2	9.7	7.5	26.7	8.8	1.4	0.4	56.5	20.3	8.9	5.2
25	Moreno Valley	19	5.9	11.3	5.6	27.2	7.1	1.7	0.6	46.4	19.8	8.2	6.3
26	Imperial Valley	21.8	8.3	13	8.4	30.6	8.4	2.1	0.9	52.3	12.1	12.3	7.8
27	Gerber	17.3	6.9	10	5.9	25.1	8	2.3	1.1	59.6	16.3	9.2	5.4
28	Carnarvon Airport	23.2	4.2	17.7	5.0	28.6	4.4	3.7	1.3	61.9	10.8	4.8	6
29	Learmonth Airport	24.8	4.9	17.9	4.9	31.9	5.6	3.3	1.2	57.4	12.3	4.1	4.8

Temperature consideration is a crucial parameter in the dry façade design process. To establish a suitable load combination relation in the design of the dry façade structure, nine configurations were considered. Table 5 presents the selected configurations as scenarios of climate change.

To illustrate the input and output data distribution based on time history, Figs. 3, 4, 5, 6, 7, and 8 depict wind speed (Ws), relative humidity (RH), minimum temperature (Min T), maximum temperature (Max T), dew point temperature (Td), and temperature (T), respectively.

Results and discussions

NARX relation

Temperature, relative humidity, and dew point temperature were trained using the NARX approach. Figure 9 displays the scatter plot between observed and predicted data for training, testing, and validation processes in scenario 1. Figures 10 and 11 show these processes for scenarios 2 and 3, respectively.

Table 4 The geographical locations of the selected weather stations

	Station#	Station name	Altitude (m)	Latitude	Longitude
Iran	1	Abadan	7	30.3473°N	48.2934°E
	2	Ahvaz	23	31.3183°N	48.6706°E
	3	Bandar Abas	10	27.1832°N	56.2666°E
	4	Bandar Lengeh	23	26.5628°N	54.8887°E
	5	Bushehr	9	28.9234°N	50.8203°E
	6	Gorgan	13	36.8456°N	54.4393°E
	7	Rasht	9	37.2682°N	49.5891°E
	8	Sari	23	36.5659°N	53.0586°E
	9	Kish Island	30	26.3156°N	53.5912°E
California (USA)	10	Atascadero	270	35.4725°N	120.6481°W
	11	King City-Oasis	91	36.1744°N	121.1172°W
	12	Lompoc	17	34.6722°N	120.5130°W
	13	Long Beach	5	33.7987°N	118.0947°W
	14	Santa Barbara	76	34.4373°N	119.7374°W
	15	Sanel Valley	168	38.9826°N	123.0893°W
	16	Santa Maria II	66	34.9134°N	120.4647°W
	17	Santa Monica	104	34.0443°N	118.4768°W
	18	Torry Pines	102	32.9018°N	117.2504°W
	19	Watsonville West II	73	36.9130°N	121.8236°W
	20	Diamond Springs	546	38.4140°N	120.4853°W
	21	Woodland	21	38.4042°N	121.4623°W
	22	Bishop	1265	37.2141°N	118.2358°W
	23	Gilroy	61	37.0010°N	121.3323°W
	24	Delano	96	35.4607°N	119.1449°W
	25	Moreno Valley	497	33.5632°N	117.1346°W
	26	Imperial Valley	47	33.2025°N	115.4320°W
	27	Gerber	69	40.0322°N	122.0900°W
AU	28	Carnarvon Airport	4	24.8831°S	113.6641°E
	29	Learmonth Airport	6	22.2312°S	114.0888°E

Table 5 Configurations of climate change

Configuration no	Input	Output	Sensitivity analysis no
1	W_s, *RH*, *Min T*, *Max T*, T_d	*T*	[SA1]
2	W_s, *RH*, T_d	*T*	[SA1]
3	*Min T*, *Max T*, T_d	*T*	[SA1]
4	T_d, *T*, W_s, *Min T*, *Max T*	*RH*	[SA2]
5	T_d, *T*, W_s	*RH*	[SA2]
6	T_d, *T*	*RH*	[SA2]
7	*RH*, *T*, *Min T*, *Max T*, W_s	T_d	[SA3]
8	*RH*, *T*, W_s	T_d	[SA3]
9	*RH*, *T*	T_d	[SA3]

It is evident from Figs. 9, 10, and 11 that configurations 1 through 3 and configurations 7 through 9 provide the closest predictions to the target. These configurations exhibit the highest level of agreement in the vicinity of the 45° line. Conversely, scenario

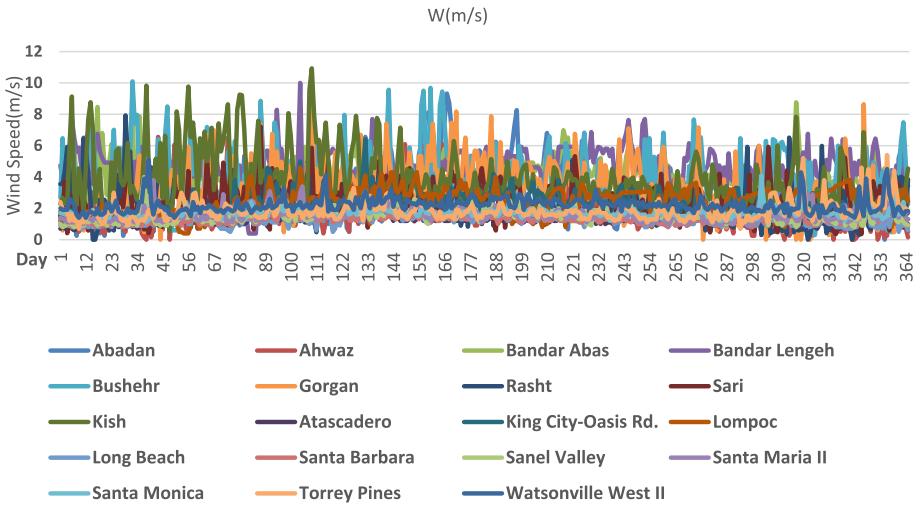

Fig. 3 Wind speed based on 365 days from various stations

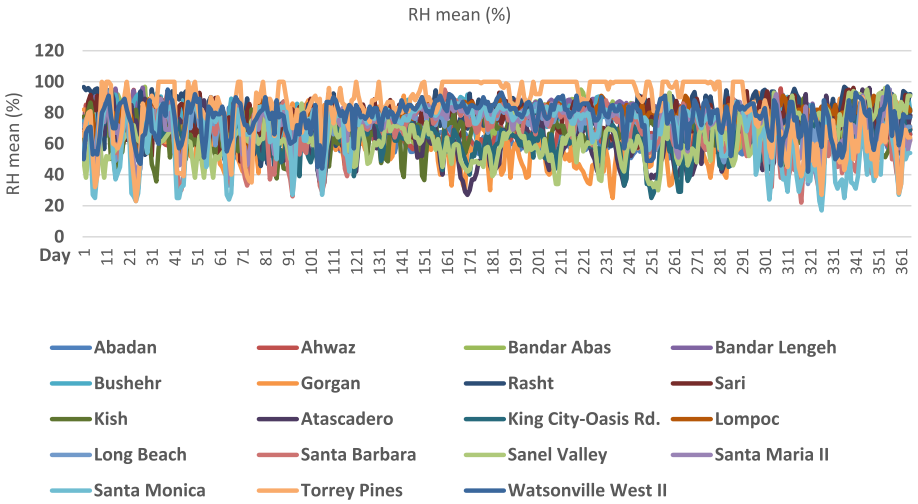

Fig. 4 Mean of relative humidity based on 365 days from various stations

2, which encompasses configurations 4 to 6, demonstrates the poorest agreement within this region. Figure 12 illustrates the number of epochs versus fitness values (RMSE) for configurations 1 through 9.

The findings presented in Fig. 10 indicate that the endeavor to attain optimal data with minimum RMSE in configurations 1, 2, 3, 7, 8, and 9 is superior to that of other configurations. Configuration 2 specifically displays a low RMSE value of only 0.442 °C and boasts superior accuracy when compared to other configurations. Statistical metric values for all configurations are provided in Table 6.

In configuration 2, the mean absolute error (MAE) and root-mean-squared error (RMSE) are both low, at 0.345 °C and 0.442 °C, respectively, while the coefficient of determination (R^2) is high at 0.998. The comparison based on *P*-value indicates that there are no significant differences between data, with a *P*-value of 0.894 which is greater than the significance level of 0.05. In scenario 2, configuration 5 stands out as the best option with a low MAE of

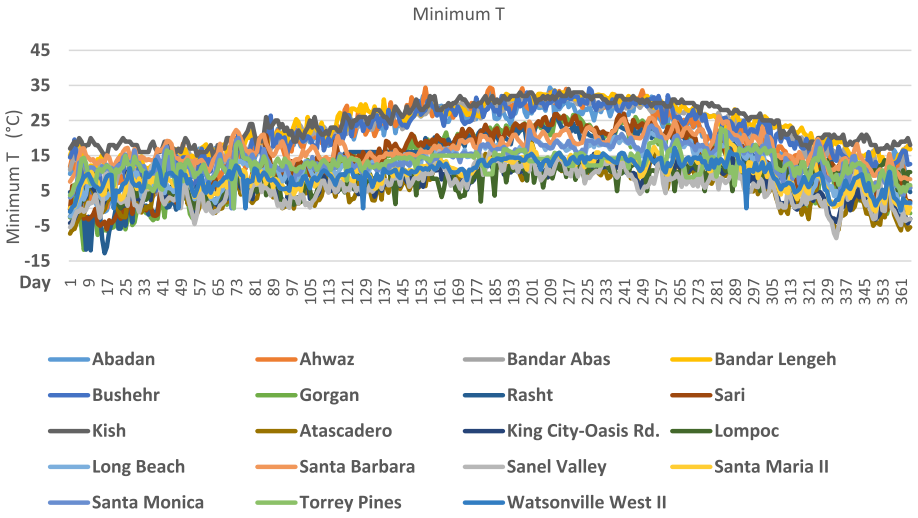

Fig. 5 Minimum of temperature based on 365 days from various stations

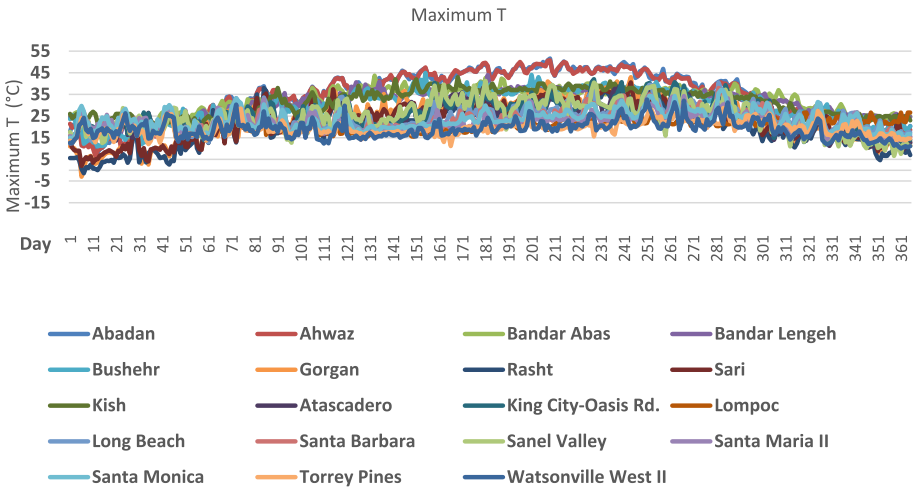

Fig. 6 Maximum of temperature based on 365 days from various stations

3.333% and RMSE of 3.907%, high R^2 of 0.977, and a *P*-value of 0.95 which is also greater than the significance level of 0.05. In scenario 3, configurations 7 to 9 exhibit accuracy levels similar to those in scenario 1. However, configuration 8 stands out with a low MAE of 0.734 °C and RMSE of 0.976 °C, high R^2 of 0.986, and a *P*-value of 0.344.

Sensitivity analysis

This study employed sensitivity analysis to evaluate the impact of each input variable on temperature (T), relative humidity (RH), and dew point temperature (Td). The aim was to determine the relative importance of each input variable including wind speed (Ws), RH, minimum temperature (Tmin), maximum temperature (Tmax), Td, and T on three different configuration scenarios with three targets. Each sensitivity test

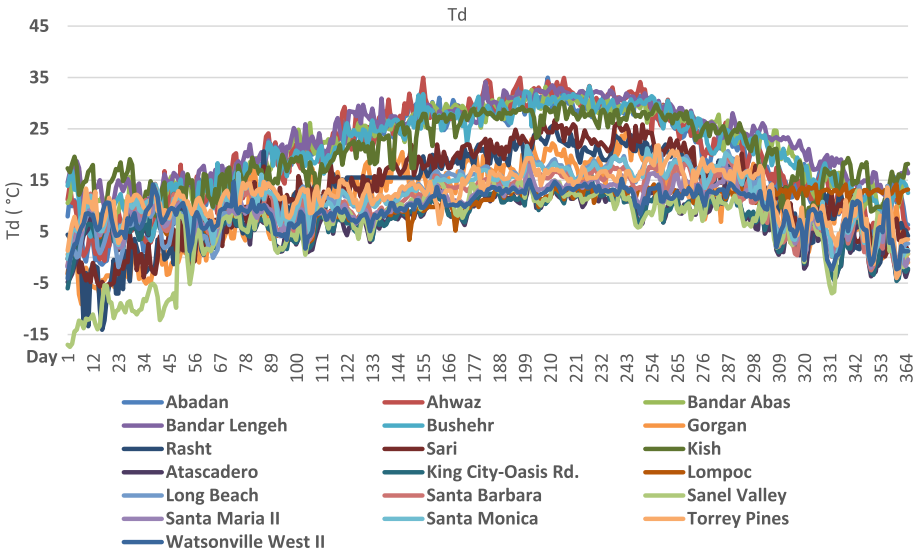

Fig. 7 Temperature of dew point based on 365 days from various stations

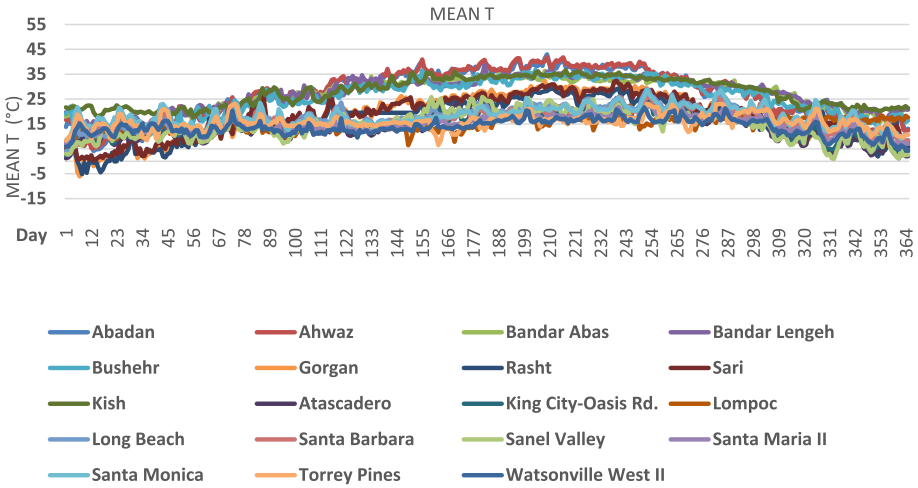

Fig. 8 Mean of temperature based on 365 days from various stations

involved varying only one input variable at a constant rate while observing its influence on T, RH, and Td at constant rates ranging from 5 to 20%. Equation 5 was used to obtain target sensitivity values by changing input variables' values at different rates. Overall, this study provides valuable insights into the impact of input variables on T, RH, and Td, which can inform the development of more accurate weather forecasting models.

$$\text{Sensitivity of } Target_{conf.} = \frac{1}{\mathrm{N}} \sum_{\mathrm{i}=1}^{\mathrm{Nt}} \left(\frac{\%\text{Change in } Target_{conf.}}{\%\text{ Change in the input variable}} \right) \times 100 \quad (5)$$

A sensitivity analysis was conducted to evaluate the relative importance of each input variable on the issue of climate change, as reported by Bateni, Vosoughifar, and Truce

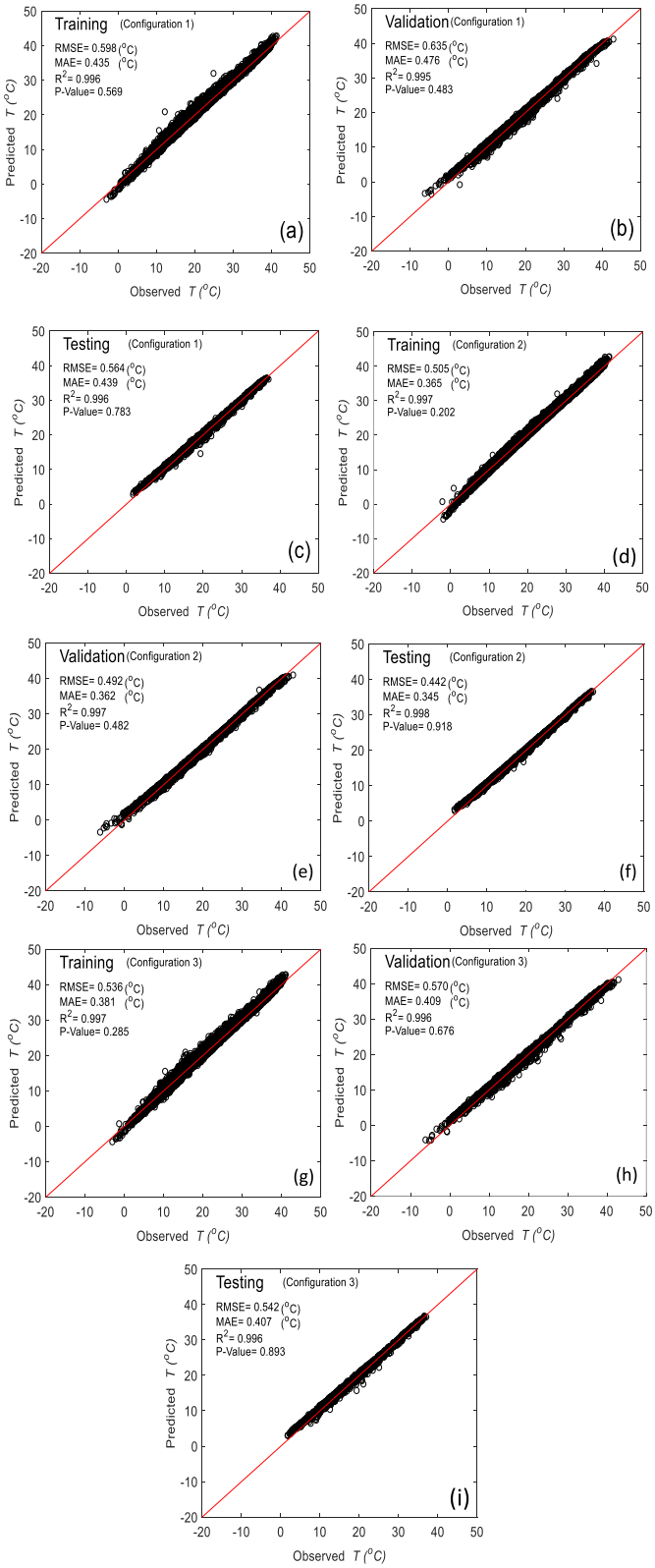

Fig. 9 Scatter plot of training, testing, validation steps, and all data for scenario 1

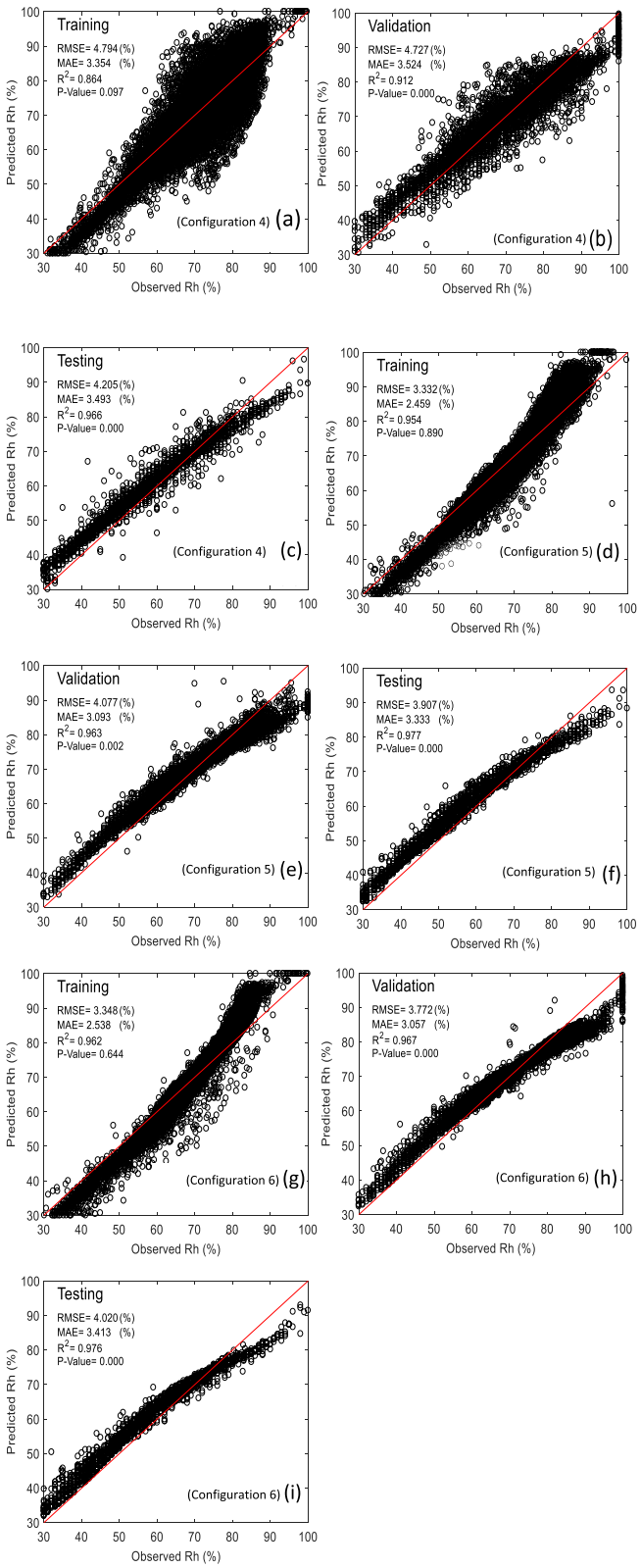

Fig. 10 Scatter plot of training, testing, validation steps, and all data for scenario 2

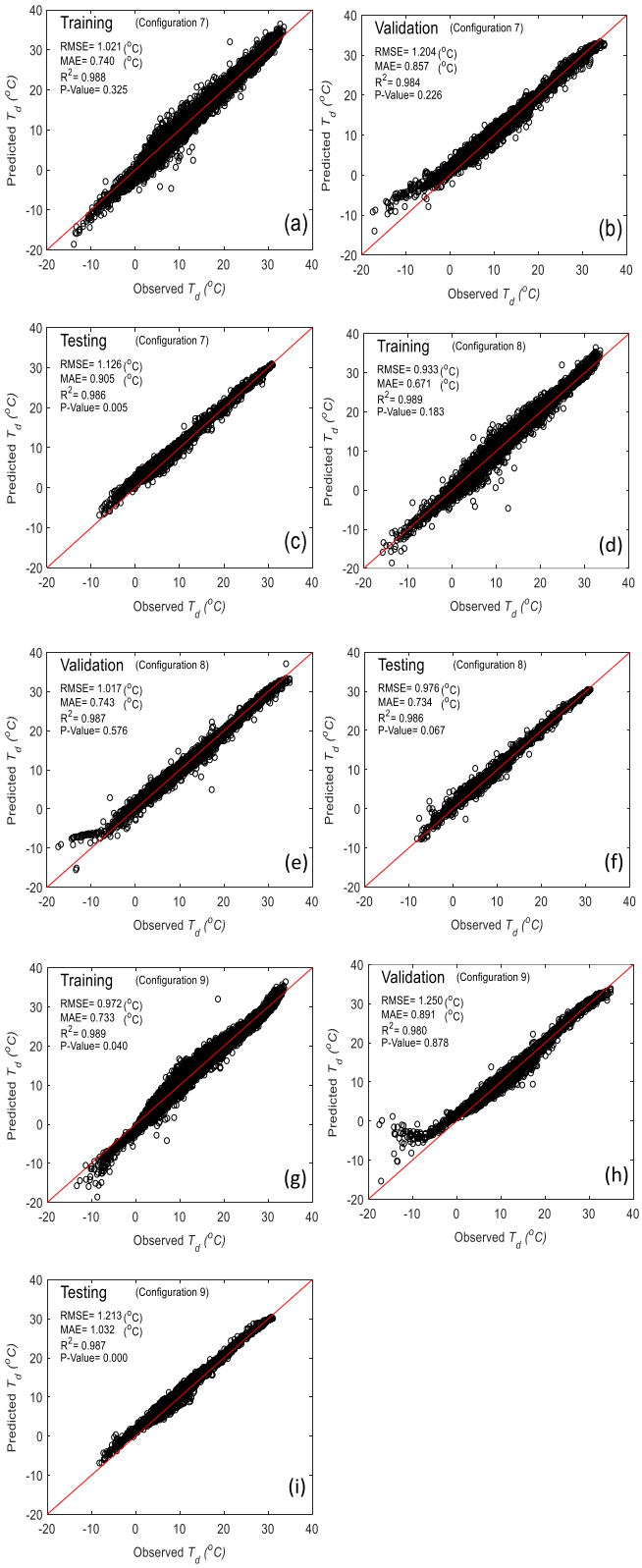

Fig. 11 Scatter plot of training, testing, validation steps, and all data for scenario 3

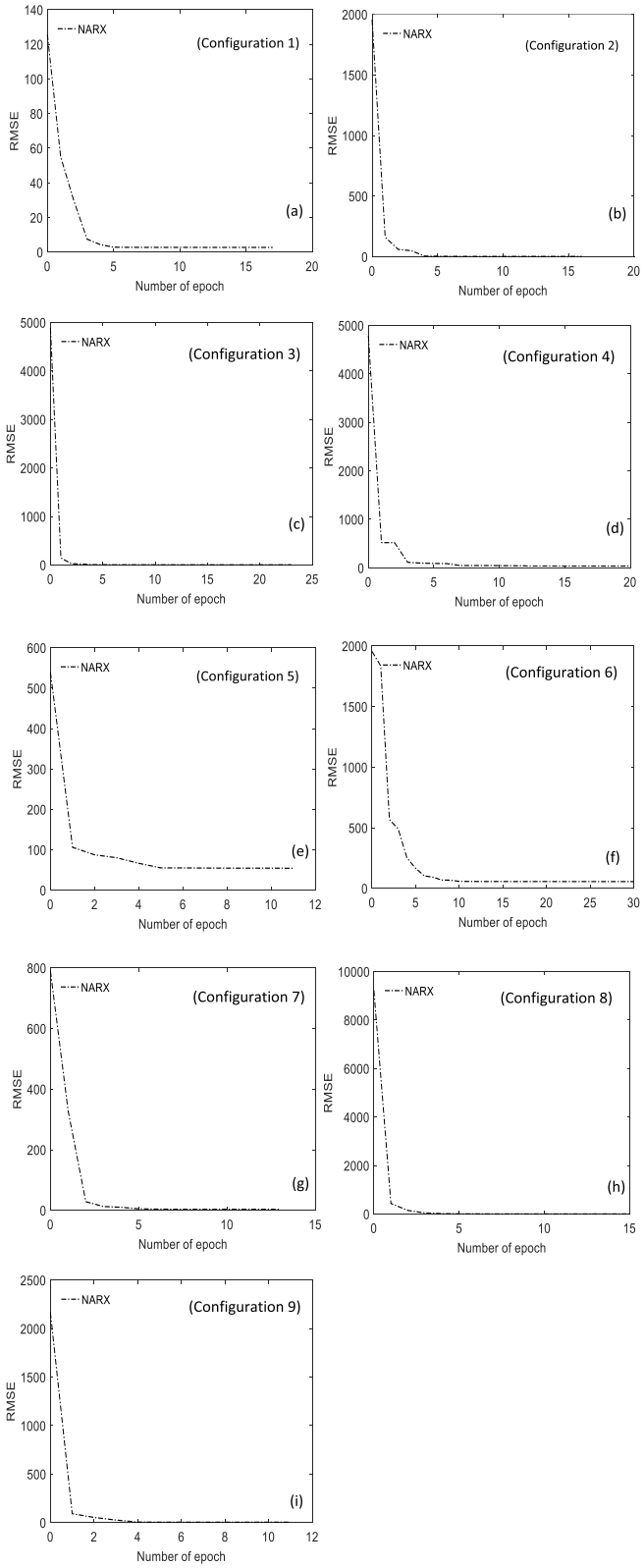

Fig. 12 Number of epoch versus fitness value (RMSE) for all configurations

Table 6 Statistical analysis of training, testing, and validation across all configurations

	Training				Validation				Testing				All data			
Configuration	**RMSE (°C)**	**MAE (°C)**	R^2	***p*-value**	**RMSE (°C)**	**MAE (°C)**	R^2	***p*-value**	**RMSE (°C)**	**MAE (°C)**	R^2	***p*-value**	**RMSE (°C)**	**MAE (°C)**	R^2	***p*-value**
1	0.598	0.435	0.996	0.569	0.635	0.476	0.995	0.483	0.564	0.439	0.996	0.783	0.603	0.443	0.996	0.822
2	0.505	0.365	0.997	0.202	0.492	0.362	0.997	0.482	0.442	0.345	0.998	0.918	0.499	0.364	0.997	0.864
3	0.536	0.381	0.997	0.285	0.570	0.409	0.996	0.676	0.542	0.407	0.996	0.893	0.543	0.388	0.997	0.453
4	4.794	3.354	0.864	0.097	4.727	3.524	0.912	0.000	4.205	3.493	0.966	0.000	4.748	3.395	0.891	0.754
5	3.332	2.459	0.954	0.890	4.077	3.093	0.963	0.002	3.907	3.333	0.977	0.000	3.521	2.632	0.960	0.950
6	3.348	2.538	0.962	0.644	3.772	3.057	0.967	0.000	4.020	3.413	0.976	0.000	3.477	2.689	0.966	0.328
7	1.021	0.740	0.988	0.325	1.204	0.857	0.984	0.226	1.126	0.905	0.986	0.005	1.065	0.772	0.988	0.054
8	0.933	0.671	0.989	0.183	1.017	0.743	0.987	0.576	0.976	0.734	0.986	0.067	0.952	0.689	0.989	0.344
9	0.972	0.733	0.989	0.040	1.250	0.891	0.980	0.878	1.213	1.032	0.987	0.000	1.045	0.781	0.987	0.019

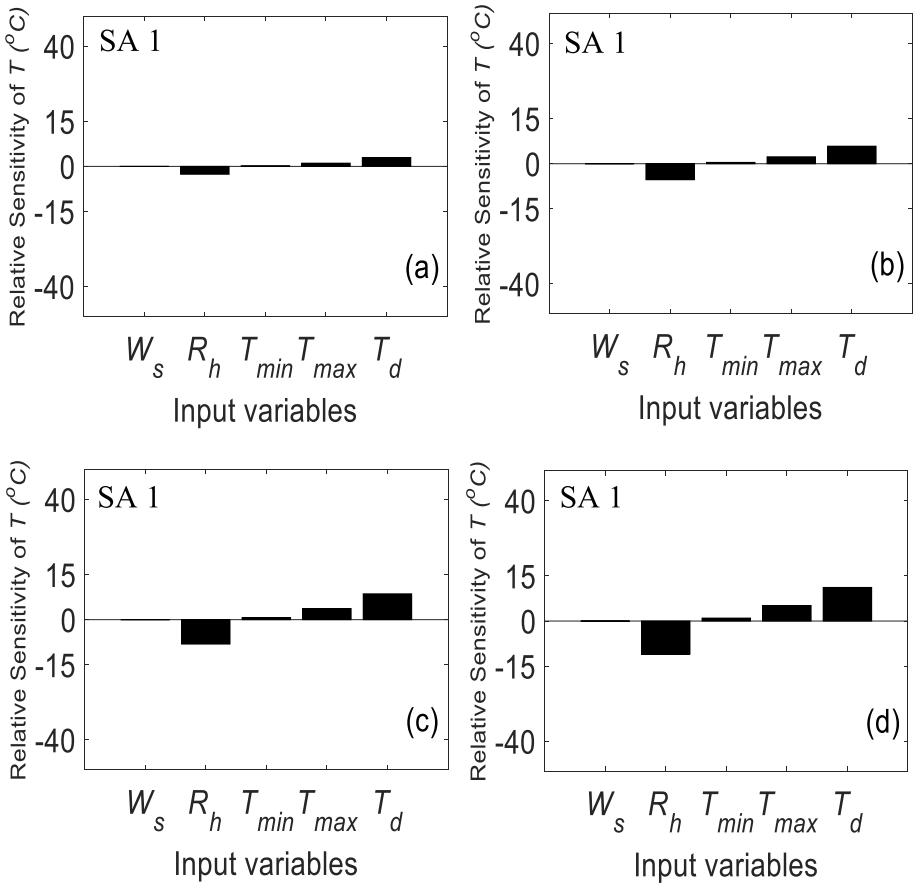

Fig. 13 Sensitivity analysis chart for configuration scenario 1

et al. [33]. Figure 13 presents the sensitivity analysis when T is the target variable, and Ws, RH, Tmin, Tmax, and Td are considered as inputs. Similarly, Fig. 14 illustrates the sensitivity analysis when RH is the target variable and Ws, T, Tmin, Tmax, and Td are considered as inputs. The results of sensitivity analysis when Td was selected as the target variable are presented in Fig. 15. Sections a, b, c, and d in Figs. 13, 14, and 15 depict an increase of 5%, 10%, 15%, and 20% in each input variable.

The findings from Fig. 13 indicate that RH and Td have the most significant impact on temperature. Specifically, RH decreases with increasing T while being inversely related to it. This relationship is evident in scenario 2 of Fig. 14 where T decreases with increasing RH due to their inverse relationship. Conversely, Td increases with increasing RH while being directly related to it. In contrast, Fig. 15 reveals that Rh and Tmax have the most significant impact on dew point temperature. Specifically, Rh and Tmax increase with increasing Td while being directly related to it.

The issue of climate change has been recognized as a crucial factor in the creation of construction quality, particularly in coastal areas, with a significant impact on occupational health and safety. Neglecting the effects of climate change can result in destructive consequences on the building's facade. Despite this, limited international efforts have been made to evaluate the preparedness of consulting and construction

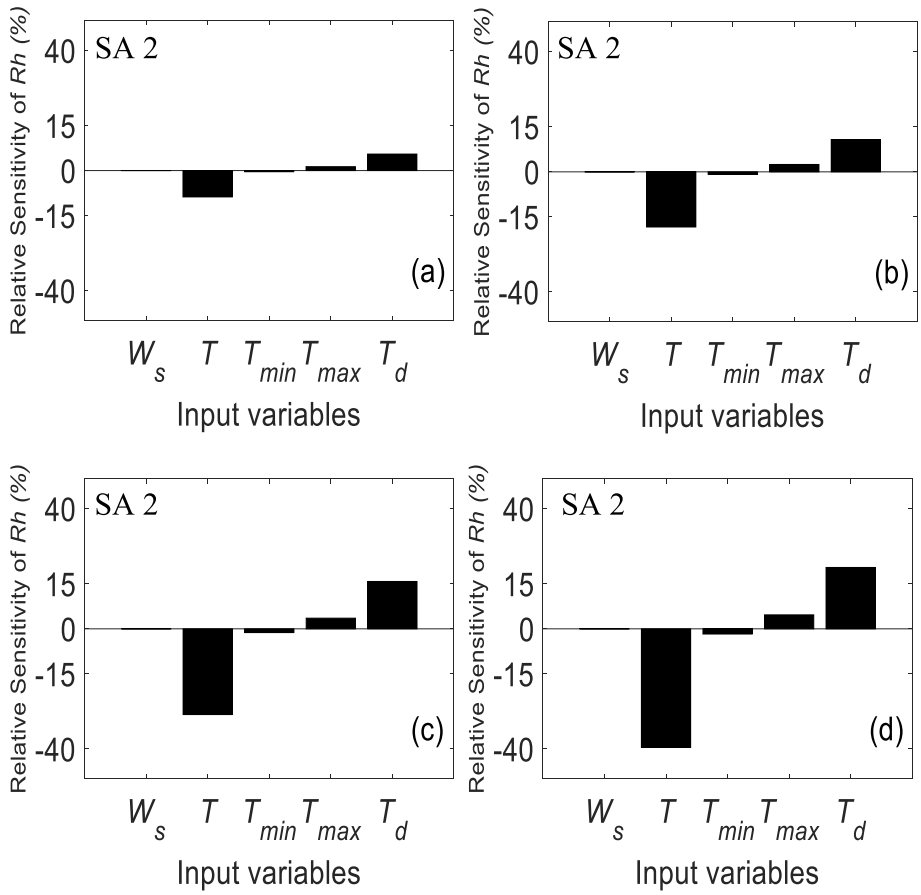

Fig. 14 Sensitivity analysis chart for configuration scenario 2

companies to adapt to climate change risks. One potential danger that may lead to the destruction of dry facades is the lack of consideration for climate change variables during the design process. The corrosion of steel elements due to relative humidity and temperature changes within a facade system can cause damage that negatively affects structural performance. To address this issue, this study selected corrosion as an important factor and utilized it as input data to consider this phenomenon within the appropriate network target. The NARX method was employed to establish a relationship between climate change data variables and their application in dry facade design. The proposed network presents a novel method for predicting temperature data in conjunction with other important variables, which can be applied to dry façade loads. One of the most critical aspects of designing a dry facade structure is determining load combinations. In traditional research and design, temperature is typically considered as the average of historical data in load combinations. However, this study recommends a modified temperature term to be included in the load combinations. This modified NARX approach offers an innovative solution for evaluating the impact of climate change on load combination in designing façade structures. By incorporating historical temperature data and other relevant variables, designers can more accurately predict future load combinations and ensure that their structures are

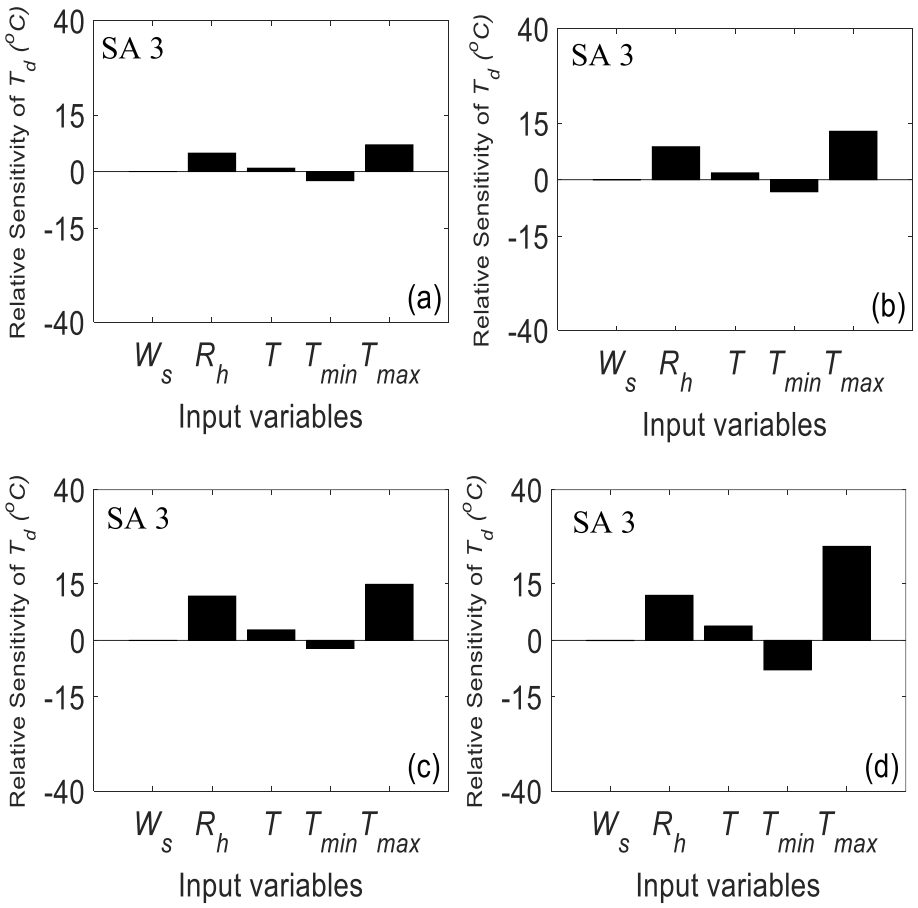

Fig. 15 Sensitivity analysis chart for configuration scenario 3

resilient to changing environmental conditions. This paper presents a detailed analysis of the proposed approach and its potential applications in the field of architecture and engineering.

Conclusions

- This study employs a comprehensive approach that takes into account various meteorological parameters, including wind speed (Ws), relative humidity (RH), minimum temperature (Tmin), maximum temperature (Tmax), and dew point temperature (Td) over a specified time period to investigate the phenomenon of climate change. The participants were categorized into nine groups.
- The results indicate that configuration 2 outperforms the other categories. This configuration exhibits a low mean absolute error (MAE) of 0.345 °C, low root-mean-square error (RMSE) of 0.442 °C, and high coefficient of determination (R^2) of 0.998. Furthermore, the P-value suggests that there are no significant differences between the data (P-value = 0.918 > 0.05).
- The findings reveal that configurations 2, 5, and 8 are the most effective configurations for scenarios 1, 2, and 3, respectively. Therefore, configurations 2, 5, and

8 can be utilized to simulate temperature, corrosion, and temperature-corrosion concurrently in load combination.

- The present research offers a significant advantage in proposing a network that can effectively respond to climate change by modifying the structure and type of system through load combination.
- This approach is particularly relevant given the current global conditions of climate change. In structural design, temperature calculations are typically based on historical data [34], with traditional analysis being recommended as a source for designing and calculating structure requirements by ASCE [14]. However, the findings of this study suggest that predicted temperature should be used in load combination instead of relying solely on average historical temperature.
- It is important to note that the proposed approach is not limited to dry facades but can be applied to many other systems where changes indicated by damage-sensitive properties are affected by climate change, such as corrosion or erosion.
- The findings of the statistical analysis tests ultimately underscore the significance of integrating climate change considerations into structural design practices. This integration is crucial in ensuring optimal performance and resilience in the face of evolving environmental conditions.

Abbreviations

ANNs	Artificial neural networks
ASD	Allowable stress design
CFS	Cold formed structure
D	Dead loads
f	Nonlinear function that can be approximated by a multilayer perceptron
L	Live loads
LRFD	Load and resistant factor design
MAE	Mean absolute error
N	Number of observations values
Nt	Number of testing data points used
NARX	Nonlinear autoregressive neural network with exogenous input
n_u	Input sequence
n_y	Output sequence
Oi	Number of observed values
Pi	Number of predicted values
P-value	Probability of comparison
R^2	Correlation coefficient
Rh	Relative humidity in percent
RMSE	Root-mean-square error
SA	Sensitivity analysis
T	Observed temperature
T_1	Temperature, creep, shrinkage loads
T_d	Dew point temperature
u(t)	Input
W_s	Wind speed
y(t)	Output
μ	Mean deviation
σ	Standard deviation

Acknowledgements

I would like to express my sincere gratitude to Dr. Vosoughifar for his tremendous support and assistance in completing this article and for providing me with an excellent opportunity to work on a project related to load combination and NARX during global climate change. Without his help and insights, completing this paper would not have been possible.

Authors' contributions

MR conceived and developed a novel idea, reviewed numerous papers, and summarized suitable ones. He also collected data, wrote, designed, and exported results from the NARX program in MATLAB.

Dr. HV analyzed and interpreted the data using the NARX method. His assistance in analyzing data played a significant role in writing the manuscript. All authors read and approved the final manuscript.

Funding
No funding was received for this study.

Availability of data and materials
The data that support the findings of this study are available from the authors upon reasonable request.

Declarations

Competing interests
The authors declare that they have no competing interests.

Received: 8 December 2022 Accepted: 14 April 2023
Published online: 25 April 2023

References

1. Paech C (2016) Structural membranes used in modern building facades. Procedia Eng 155:61–70. https://doi.org/10.1016/J.PROENG.2016.08.007
2. Badr AR, Elanwar HH, Mourad SA (2019) Numerical and experimental investigation on cold-formed walls sheathed by fiber cement board. J Constr Steel Res 158:366–380. https://doi.org/10.1016/J.JCSR.2019.04.004
3. Eisenberg DA (2016) Transforming building regulatory systems to address climate change. Http://Dx.Doi.Org/10.1080/09613218.2016.1126943 44(5–6):468–473. https://doi.org/10.1080/09613218.2016.1126943
4. Lacasse MA, Gaur A, Moore TV (2020) Durability and Climate Change—Implications for Service Life Prediction and the Maintainability of Buildings. National Research Council Canada, Construction Research Centre, 1200 Montreal Road, Building M24, Ottawa, ON K1A 0R6, Canada. Buildings 10(3):53. https://doi.org/10.3390/buildings10030053
5. Van Den Bossche N, Janssens A, Moore T, Lacasse M (2020) Development of numerical model for determination of pressure equalization in facades during wet conditions. Build Environ 178:106919. https://doi.org/10.1016/J.BUILDENV.2020.106919
6. Hurlimann AC, Warren-Myers G, Browne GR (2019) Is the Australian construction industry prepared for climate change? Build Environ 153:128–137. https://doi.org/10.1016/J.BUILDENV.2019.02.008
7. Yau YH, Hasbi S (2013) A review of climate change impacts on commercial buildings and their technical services in the tropics. Renew Sustain Energy Rev 18:430–441. https://doi.org/10.1016/J.RSER.2012.10.035
8. Nguyen MN, Leicester RH, W CH (2008) Climate change: implications for buildings. Key findings... - Google Scholar. Service life models for timber structures protected in building envelope, CSIRO Sustainable ecosystems. https://scholar.google.com/scholar?Lookup=0&q=climate+change:+implications+for+buildings.+Key+findings+from+the+intergovernmental+panel+on+climate+change+Fifth+Assessment+Report+P+Chalmers+-+World+Business+Council+for+Sustainable+Development+…,+2014&hl=en
9. Du J, Wang H, Wang S, Song X, Wang J, Chang A (2020) Fatigue damage assessment of mooring lines under the effect of wave climate change and marine corrosion. Ocean Eng 206:107303. https://doi.org/10.1016/j.oceaneng.2020.107303
10. Jimenez-Martinez M (2021) Harbor and coastal structures: a review of mechanical fatigue under random wave loading. Heliyon 7(2021):e08241. https://doi.org/10.1016/j.heliyon.2021.e08241
11. Soufeiani L, Foliente G, Nguyen KTQ, San Nicolas R (2020) Corrosion protection of steel elements in façade systems – a review. J Build Eng 32:101759. https://doi.org/10.1016/J.JOBE.2020.101759
12. Lisø KR (2011) Integrated approach to risk management of future climate change impacts. Http://Dx.Doi.Org/10.1080/09613210500356022 34(1):1–10. https://doi.org/10.1080/09613210500356022
13. Lisø KR, Aandahl G, Eriksen S, Alfsen KH (2003) Preparing for climate change impacts in Norway's built environment. Build Res Inf 31(3–4):200–209. https://doi.org/10.1080/0961321032000097629
14. American Society of Civil Engineers Minimum Design Loads for Buildings and Other Structures, ASCE STANDARD (2020) ASCE 7-10 ASD Load Combinations. Chapter 2, Combinations of loads. ISBN 978-0-7844-1085-1 (alk. paper)
15. Yang T, Sun F, Gentine P, Liu W, Wang H, Yin J, Du M, Liu C (2019) Evaluation and machine learning improvement of global hydrological model-based flood simulations. Environ Res Lett 14(11). https://doi.org/10.1088/1748-9326/AB4D5E
16. Lee J, Kim CG, Lee JE, Kim NW (2018) Kim H Application of artificial neural networks to rainfall forecasting in the Geum River Basin, Korea. Water 10(10):1448. https://doi.org/10.3390/W10101448
17. Zou Q, Xiong Q, Li Q, Yi H, Yu Y, Wu C (2020) A water quality prediction method based on the multi-time scale bidirectional long short-term memory network. Environ Sci Pollut Res 27(14):16853–16864. https://doi.org/10.1007/S11356-020-08087-7
18. AltanDombayci Ö, Gölcü M (2009) Daily means ambient temperature prediction using artificial neural network method: a case study of Turkey. Renew Energy 34(4):1158–1161. https://doi.org/10.1016/J.RENENE.2008.07.007
19. Di Nunno F, Granata F (2020) Groundwater level prediction in Apulia region (Southern Italy) using NARX neural network. Environ Res 190:110062. https://doi.org/10.1016/J.ENVRES.2020.110062
20. Shahbaz M, Taqvi SAA, Inayat M, Inayat A, Sulaiman SA, McKay G, Al-Ansari T (2020) Air catalytic biomass (PKS) gasification in a fixed-bed downdraft gasifier using waste bottom ash as catalyst with NARX neural network modelling. Comput Chem Eng 142:107048. https://doi.org/10.1016/J.COMPCHEMENG.2020.107048
21. Sum JPF, Kan WK, Young GH (2014) A note on the equivalence of NARX and RNN. Neural Comput Appl 1999 8:1, 8(1), 33–39. https://doi.org/10.1007/S005210050005

22. Ezzeldin R, Hatata A (2018) Application of NARX neural network model for discharge prediction through lateral orifices. Alex Eng J 57(4):2991–2998. https://doi.org/10.1016/J.AEJ.2018.04.001
23. O'Neill BC, Carter TR, Ebi K, Harrison PA, Kemp-Benedict E, Kok K, Kriegler E, Preston BL, Riahi K, Sillmann J, van Ruijven BJ, van Vuuren D, Carlisle D, Conde C, Fuglestvedt J, Green C, Hasegawa T, Leininger J, Monteith S, Pichs-Madruga R (2020) Achievements and needs for the climate change scenario framework. Nat Clim Change 10(12):1074–1084. https://doi.org/10.1038/s41558-020-00952-0
24. Van Vuuren DP, Riahi K, Moss R, Edmonds J, Thomson A, Nakicenovic N, Kram T, Berkhout F, Swart R, Janetos A, Rose SK, Arnell N (2012) A proposal for a new scenario framework to support research and assessment in different climate research communities. Glob Environ Chang 22(1):21–35. https://doi.org/10.1016/J.GLOENVCHA.2011.08.002
25. Grant N, Hawkes A, Napp T, Gambhir A (2020) The appropriate use of reference scenarios in mitigation analysis. Nat Clim Change 2020 10:7, 10(7), 605–610. https://doi.org/10.1038/s41558-020-0826-9
26. Bateni SM, Vosoughifar H, Ek MB, Xu T, Bateni SM, Vosoughifar H, Ek MB, Xu T (2019) Estimation of daily reference evapotranspiration from limited climatic variables in coastal regions. AGUFM, 2019, H31L-1880. https://ui.adsabs.harvard.edu/abs/2019AGUFM.H31L1880B/abstract
27. Adda J, Gonzalo J (1996) *P*-values for non-standard distributions with an application to the DF test. Econ Lett 50(2):155–160. https://doi.org/10.1016/0165-1765(95)00741-5
28. Baduashvili A, Evans AT, Cutler T (2020) How to understand and teach P values: a diagnostic test framework. J Clin Epidemiol 122:49–55. https://doi.org/10.1016/J.JCLINEPI.2020.03.003
29. Evapotranspiration (n.d.) Retrieved September 9, 2021, from http://www.bom.gov.au/watl/eto/maps/aus.shtml
30. CIMIS (n.d.) Retrieved September 9, 2021, from https://cimis.water.ca.gov/
31. I.R. of Iran Meteorological Organization (IRIMO) | E-Library (n.d.) Retrieved September 9, 2021, from https://library.wmo.int/index.php?lvl=author_see&id=11237
32. Google Earth (n.d.) Retrieved September 9, 2021, from https://earth.google.com/web/
33. Bateni SM, Vosoughifar HR, Truce B, Jeng DS (2019) Estimation of clear-water local scour at pile groups using genetic expression programming and multivariate adaptive regression splines. J Waterw Port Coast Ocean Eng 145(1):04018029. https://doi.org/10.1061/(ASCE)WW.1943-5460.0000488
34. Reksowardojo AP, Senatore G, Smith IFC (2020) Design of structures that adapt to loads through large shape changes. J Struct Eng 146(5):04020068. https://doi.org/10.1061/(ASCE)ST.1943-541X.0002604

Publisher's Note